Institute of Paper Science and Technology
Atlanta, Georgia

IPST Technical Paper Series Number 937

Electron Microscopy

D.R. Rothbard and J.G. Sheehan

March 2002

Submitted as Book Chapter
in
The Paint and Coating Testing Manual

INSTITUTE OF PAPER SCIENCE AND TECHNOLOGY
PURPOSE AND MISSIONS

The Institute of Paper Science and Technology is an independent graduate school, research organization, and information center for science and technology mainly concerned with manufacture and uses of pulp, paper, paperboard, and other forest products and byproducts. Established in 1929 as the Institute of Paper Chemistry, the Institute provides research and information services to the wood, fiber, and allied industries in a unique partnership between education and business. The Institute is supported by more than 40 member companies. The purpose of the Institute is fulfilled through four missions, which are:

- to provide a multidisciplinary graduate education to students who advance the science and technology of the industry and who rise into leadership positions within the industry;
- to conduct and foster research that creates knowledge to satisfy the technological needs of the industry;
- to provide the information, expertise, and interactive learning that enable customers to improve job knowledge and business performance;
- to aggressively seek out technological opportunities and facilitate the transfer and implementation of those technologies in collaboration with industry partners.

ACCREDITATION

The Institute of Paper Science and Technology is accredited by the Commission on Colleges of the Southern Association of Colleges and Schools to award the Master of Science and Doctor of Philosophy degrees.

NOTICE AND DISCLAIMER

The Institute of Paper Science and Technology (IPST) has provided a high standard of professional service and has put forth its best efforts within the time and funds available for this project. The information and conclusions are advisory and are intended only for internal use by any company who may receive this report. Each company must decide for itself the best approach to solving any problems it may have and how, or whether, this reported information should be considered in its approach.

IPST does not recommend particular products, procedures, materials, or service. These are included only in the interest of completeness within a laboratory context and budgetary constraint. Actual products, materials, and services used may differ and are peculiar to the operations of each company.

In no event shall IPST or its employees and agents have any obligation or liability for damages including, but not limited to, consequential damages arising out of or in connection with any company's use of or inability to use the reported information. IPST provides no warranty or guaranty of results.

Publication Information

Title of Paper:
Chapter 72 – Electron Microscopy

Paper ID No.:
10268

Authors:
David R. Rothbard
Institute of Paper Science and Technology, 500 10th Street, NW, Atlanta, GA 30318
John G. Sheehan
Bristol-Myers Squibb, 1000 Stewart Avenue, Garden City, NY 11530

Title of Book:
Manual 17
The Paint and Coating Testing Manual
15th Edition of the Gardner-Sward Handbook

Book Editor:
Joseph V. Koleske

Publisher:
American Society for Testing and Materials
ASTM International
West Conshohocken, PA

Submission Deadline:
March 29. 2002

72

Electron Microscopy

by David R. Rothbard[1] and John G. Sheehan[2]

INTRODUCTION

Electron microscopes are frequently used in the analysis of coatings and their components because of their high resolution and multifunctional capabilities. The two common types are the scanning electron microscope (SEM) and the transmission electron microscope (TEM). In various operating modes and with specialized detectors these instruments can be used to examine surface texture and internal structure, determine particle size and shape, provide elemental analysis, and reveal crystallographic orientation and identity.

The resolving power of electron microscopes is orders of magnitude greater than that of light-optical microscopes, partly due to the shorter electromagnetic wavelength (higher energy) of electron illumination. Modern SEMs with field-emission electron guns have the ability to resolve better than 1 nm between objects and commercial TEMs can resolve better than 0.2 nm. However, the actual resolution obtained is highly dependent on the nature and preparation of the sample. Contrast develops in SEM by electrons emitted at or near the surfaces of bulk specimens and therefore topography and composition are examined. Contrast develops in TEM by electrons transmitted through thin specimens and therefore variations in structure and composition are examined. Due to the improved resolution of modern SEMs, TEMs are no longer needed to see coating components 50 nm or smaller. In this chapter, SEM will receive more attention than TEM for this reason, along with its greater availability and documented coatings applications.

Types of signals generated in a sample by a vertically incident electron beam are illustrated in Figure 1. An SEM typically has detectors for secondary electrons (SE), backscattered electrons (BSE), and X rays, positioned above the surface of bulk specimens. The TEM collects elastically and inelastically scattered electrons, and sometimes X rays, from thin (ca. 100 nm) specimens. Hybrid TEMs have some SEM capabilities. They may collect BSEs and SEs from the incident-beam side of thin specimens, a variety of transmitted electron signals from the opposite side of the sample, and X rays from both sides. These are known as scanning transmission electron microscopes (STEM) or analytical electron microscopes (AEM). Their greatest strength is their ability to focus a fine electron probe on very thin samples, achieving high spatial resolution in elemental and structural analysis.

SEM and TEM were both invented in the 1930s in Germany [*1*]. Ernst Ruska shared the 1986 Nobel Prize in Physics for designing the transmission electron microscope and improving

[1] Institute of Paper Science and Technology, 500 10th Street, NW, Atlanta, GA 30318.

[2] Bristol-Myers Squibb Company, 1000 Stewart Avenue, Garden City, NY 11530.

electron optics. Soon after its invention, TEM became widely used to image replicas of surfaces at resolution far better than was possible with the first SEM and therefore further development of SEM continued at a slow pace. An important step was the invention of an efficient secondary electron detector by Everhart and Thornley in 1960. In 1965; the Cambridge Instrument Company introduced the first commercial SEM. SEM was quickly applied to the study of coatings, as evidenced by American Chemical Society Symposia on SEM of polymers and coatings in 1970 [*2*] and 1973 [*3*].

Some of the greatest recent improvements in SEM design and operation were made possible by the rapidly increasing power and decreasing cost of personal computers. Manufacturers (and after-market suppliers) have moved to using standard personal computer (PC) interfaces and operating systems to control microscope functions. These range from alignment and focusing to digital image collection and processing. Intensive image processing and crystallographic computations are performed quickly during an imaging session. A single PC can integrate these and other functions, such as energy dispersive spectrometer (EDS) analysis and motor stage control. This has simplified SEM and TEM operation. By accessing the PC remotely, service problems can be diagnosed before a service engineer is sent.

This chapter has three main parts: SEM, TEM, and further applications to coatings. The SEM section begins with a description of the electron-optical column including the electron gun, lens system, and scan coils. This is followed by a discussion of image formation and signal collection. The function of these components must be understood in order to create ideal operating conditions for SEM and to correctly interpret SEM images. Also included is a discussion of X-ray microanalysis, used to identify and measure the elements present in a sample. The SEM section also has an overview of sample preparation, including conductive coatings and cross-section analysis. In the TEM section is a brief discussion of contrast and electron optics. The last section discusses some additional applications of electron microscopy to coatings, from pigment sizing and identification to structure and wear.

SCANNING ELECTRON MICROSCOPY

The main specifications that control the performance of an SEM are the type of electron gun and whether the sample chamber will have variable pressure capabilities (in addition to the standard high-vacuum sample environment). In configuring an SEM, there are a wide variety of choices in signal detection systems. These have to be balanced against the size and geometry of the sample chamber. Vacuum systems for SEMs have become more complex due to the need for higher vacuum in the electron gun and lower (weaker) vacuum levels in the sample chamber.

The SEM can image surfaces at magnifications from about 10 to 200 000 times. Depth of focus is large, so rough surfaces may be fully focused. The types of signals that can be collected include secondary electrons (SE), backscattered electrons (BSE), and characteristic X rays. As the electron beam scans the sample, the signal from each spot is collected, amplified, and synchronously displayed on the monitor with an intensity proportional to the collected signal. The same scan generator deflects the electron beam across both the sample and the monitor and therefore the image displayed is a magnified view of the scanned area. In digital SEMs, the scans are digitally stepped with control over step size and dwell time per pixel.

To clearly see a feature of interest requires sufficient contrast, magnification, and resolution. Each of the signal types noted above has its own contrast mechanisms. Although SEMs

commonly have magnification ranges above 100 000 times, no useful image can be obtained unless fine enough resolution exists. Spatial resolution is the ability to differentiate two closely spaced objects, measured by their distance of separation. An instrument with 3 nm spatial resolution will not provide sharp images of 3 nm objects. Instead, it will be able to differentiate larger objects spaced as closely as 3 nm apart, if they respond ideally under the electron beam.

A schematic diagram of the SEM is shown in Figure 2. Electrons are drawn out of the gun by the electric field between the source and the anode. The condenser lenses form the beam into a finely focused probe. The scan coils cause the probe to scan across the sample in a raster. The final lens focuses the beam on the sample. Any combination of BSE, SE, and characteristic X rays can be detected. Details of the function of each component in the SEM are discussed below.

Electron Guns

The ultimate resolution of an ideal sample imaged in the SE mode of SEM is substantially controlled by the type of cathode in the electron gun, or source. The resolution is improved by making the probe diameter at the specimen surface smaller. This beam diameter can be expressed in nanometers as

$$d_{min} = K\, C_s^{1/4}\, \lambda^{3/4}\, (1+i_p/B\lambda^2)^{3/8}$$

where K is a constant near one, C_s is the spherical aberration of the lens, λ is the electron wavelength in nanometers, i_p is the probe current in amperes, and B is the electron gun brightness (in amperes per centimeter squared – steradian) [*5*]. To decrease the beam diameter (improving resolution) one can use an electron gun with higher brightness (current density). In any SEM, lowering the probe current (using condenser lens controls) and decreasing wavelength (by increasing accelerating voltage) should decrease probe size.

An SEM can be designated conventional or field emission (abbreviated FESEM or FEG SEM), depending on which gun type is incorporated. Characteristics of electron sources are summarized in Table 1. A conventional SEM may have either a tungsten filament or a lanthanum hexaboride (LaB_6) crystal cathode, the most common thermionic cathode materials. Thermionic excitation occurs when a filament is heated to near its melting point, allowing electrons to overcome their work function and eject themselves into the vacuum. Tungsten cathodes consist of a wire bent like a hairpin. They are easy to operate and need only moderate vacuum to prevent oxidation. However, they require frequent replacement (ca. 50-100 hours). LaB_6 cathodes consist of a crystal of that compound soldered directly to refractory metal strips or with an intermediate carbon-ceramic support. Compared to tungsten, LaB_6 has higher current density, and a smaller diameter of the first crossover, resulting in better resolution (Table 1). Another advantage of LaB_6 cathodes is their significantly longer lifetimes. However, LaB_6 guns require somewhat higher vacuum to slow evaporation from reactions of LaB_6 with oxygen-containing residual gases [*6*]. This adds to the expense and complexity of the gun vacuum system.

Field emission electron guns deliver orders of magnitude higher current density (brightness) than conventional SEM sources, but require a larger capital investment. FESEMs are made with either cold or thermal field emission design. Field emission occurs when a huge potential gradient ($>10^7$ V/m) is applied to a tungsten tip of about 0.1 μm in diameter, causing electrons to tunnel through their potential barrier. No thermal energy is needed to lift the electrons over the

barrier. The combination of high current density and small diameter of the first crossover in FE guns makes possible ultrahigh resolution (<1 nm) SEM imaging. The diameter of the first crossover from a field emitter is only about 10 nm and therefore only one condenser lens is needed to demagnify the probe enough for high-resolution imaging. Gas molecules that strike the tip cause the work function to rise and the emission to fall. Field emitters that operate at room temperature (known as "cold field" emitters) require vacuum better than 10^{-8} Pa. Even in a clean vacuum, gas molecules eventually cover the tip. The tip is cleaned by rapid heating (flashing) at about 2300 K.

A second type of high current density source is thermal field emission, including the Schottky design. This cathode contains a zirconium oxide (ZrO) coated tungsten crystal maintained at 1800 K. The high temperature avoids the flashing required to clean cold FE tips and accommodates a slightly weaker gun vacuum. The ZrO coating lowers the work function, easing electron emission [5]. Schottky emitters can produce higher beam currents, valuable in some backscattering and x-ray analysis applications.

SEM at low accelerating voltages (below 5 kV) has the advantages of less specimen damage and less surface-charge buildup. There is improved representation of surface details because the primary electron beam does not penetrate as deeply, and there is a smaller region of secondary electron emission. Until recently, low-voltage SEM was limited in resolution mainly by large chromatic aberrations in final lenses, which arise from the large energy spread of electron beams from thermionic cathodes. This problem has been overcome by FE cathodes, whose energy spread is an order of magnitude smaller than in thermionic cathodes (Table 1). The merits of low-voltage SEM for surface imaging and EDS were discussed by Boyes [7].

Magnetic Lenses and Scan Coils

The purpose of the condenser lens system in the SEM is to deliver electrons from the first crossover to the specimen plane in a small-diameter, high-intensity beam. SEMs with thermionic electron guns have two demagnifying condenser lenses plus a final condenser lens (Figure 2). The first condenser is placed halfway between the second condenser and the electron gun, and the second is placed halfway between the gun and the specimen. Two condenser lenses instead of one are advantageous because more electrons are collected and focused into the probe, and the probe diameter is smaller. The spray aperture in each condenser lens intercepts scattered electrons and decreases spherical aberrations. The first spray aperture is usually fixed and the final aperture is selectable to varying diameters. While a smaller probe diameter improves resolution, it is not always advantageous because it reduces both the probe current and the signal-to-noise ratio. Higher probe currents are needed for EDS and some BSE detectors. The operator must decide which combination of aperture and condenser lens currents fits the requirements of resolution and signal detection.

The lens closest to the sample is often incorrectly called the "objective" lens. It is more accurately called the final condenser lens. There is no objective lens in an SEM because, unlike a TEM and compound light microscope, all SEM lenses are on the same side of the sample as the illumination source (electron gun). The purpose of the final lens is to provide the operator with a fine control for the focus of the beam at the sample surface.

The scan coils, located within or above the final lens, deflect the electron beam across the sample in a raster pattern. The image signal from a selected detector is simultaneously displayed

on the monitor in the same positional coordinate system. Magnification is the ratio of a feature's length in the image to the length of the beam deflection across that feature in the sample. The distance between the bottom of the final lens and the top of the sample is known as the working distance. The depth of focus is inversely proportional to the working distance. Probe diameters are small when the beam is focused at short working distances. Therefore, high-magnification imaging should be done at short working distances and low-magnification imaging should be done at long working distances (if more depth of focus is desired).

Image Formation

Most SEMs are equipped to detect secondary electrons (SE), backscattered electrons (BSE), and characteristic X rays as the electron beam scans across sample surfaces. The SE signal is produced when bound electrons are removed as a result of inelastic scattering of the electron beam. The intensity of the SE signal depends partly on the orientation of the sample with respect to the electron beam, which is why SE images have topographic contrast. X-ray detection is discussed in a later section.

Backscattered electrons (BSE) result from elastic scattering of the primary electron beam. Electrons are elastically scattered when they penetrate the electron clouds of target atoms and change direction without losing energy. An electron is backscattered after a series of direction-changing elastic events that cause the electron to exit the sample. The probability of a backscatter event depends on the size of the nuclei and therefore backscatter contrast depends on the distribution of average atomic number in the sample. BSE images of flat specimens show higher atomic number phases as brighter. The depth in a sample from which BSE information emerges ranges from about 80 nm for gold to about 600 nm for aluminum if the accelerating potential is 20 kV [*6*]. Since BSEs can come from deeper in the sample (lower in the teardrop in Figure 1), the spatial resolution is generally poorer than in SE images. The BSE signal strength drops rapidly below 10 kV and its behavior changes significantly below 5 kV.

Although some BSEs reach the Everhart-Thornley detector used for SE collection, it is an inefficient way to collect them. BSE detectors are generally either of the solid-state or scintillator design. They are retractable or permanently mounted above the sample (labeled "BE Detector" in Figure 2). A solid-state detector is a disk-shaped detector placed just below final lens with a hole in the center for the electron beam. Scintillator-type detectors have an aluminized layer on a light pipe connected to a photomultiplier. They take up more space but respond better at fast scan rates.

Most SEM images are acquired with secondary electrons using the Everhart-Thornley (ET) detector, shown in Figure 3. SEs have low energy (<50 eV) and escape from the near-surface to provide more surface-sensitive data with higher resolution than BSEs. The ET detector collects mainly SEs, with a small contribution of BSEs. The major components of the ET detector are a collector grid, a scintillator, and a photomultiplier. SEs are pulled toward the scintillator by a small positive potential on the collector grid. A 10 to 12 kV bias on the scintillator coating accelerates SEs enough to cause photon emission when they strike the scintillator.

Secondary electrons are classified into four types, shown schematically in Figure 3. SE1s are generated by direct interaction with the primary beam and therefore carry the highest resolution information. SE2s are generated by backscattered electrons as they exit the sample surface and therefore contribute subsurface atomic number contrast. Since SE2s come from a

large electron diffusion zone around the primary beam, they degrade spatial resolution. In 1940, before the first SEM images were collected, von Ardenne correctly predicted that SE2s would limit resolution [*1*]. SE2s cannot be detected separately from SE1s, but operating parameters (like lower accelerating potential) can lower their contribution.

SE3s are generated by backscattered electrons that strike the final lens pole piece and the specimen chamber walls. SE4s are generated when the primary beam strikes internal column parts. SE3s generated at the final lens pole piece can be reduced with a shield made of low SE-emitting material, such as carbon-coated aluminum, placed just below the final lens. A +50 V bias applied to the shield prevents the escape from the shield of any SE3s. To increase atomic number contrast, BSEs that strike the shield can be converted into SEs when the shield is positively biased or covered with a material that emits a large number of secondary electrons. Reimer [*6*] discussed these signal types in detail. Peters [*8*] reviewed procedures for high-resolution SE image formation.

To demonstrate the importance of understanding how SE1, SE2, SE3, and BSE generate contrast in the SEM, three micrographs of the same area of a 1:6 styrene-butadiene latex to calcium carbonate coating formulation (air-dried from 80 wt%) are shown in Figure 4. Micrographs in Figures 4A and 4B were recorded at 20 and 5 kV, respectively, with an Everhart-Thornley detector. In Figure 4A, the calcium carbonate particles are visible from beneath the latex-film surface from a combination of SE2, SE3, and BSE. This is possible because the exit depth of BSE from a latex film is about 1 μm at 20 kV. In Figure 4B, the calcium carbonate particles are barely visible because the exit depth of BSE, and therefore contrast from SE2 and SE3, is less than 100 nm at 5 kV. Comparison of Figures 4A and 4B demonstrates the strong dependence of accelerating voltage on the appearance of SEM images. Sometimes more than one accelerating voltage is needed for correct interpretation. SE images at lower accelerating voltage better represent topography because the exit depth of BSEs (generating SE2s) is smaller.

The micrograph in Figure 4C shows the same area as Figures 4A and 4B, this time recorded with an annular solid-state BSE detector. Since no SEs were detected, the latex binder at the sample surface generated no contrast. Instead, contrast was generated by the distribution of calcium carbonate particles beneath the latex-film surface. This example illustrates the importance of understanding signal generation in the SEM in order to correctly interpret images. Observation of only Figure 4A would lead one to the false conclusion that the latex film does not cover all of the calcium carbonate particles.

X-Ray Microanalysis

Inner shell ionization is the event that triggers characteristic X-ray production. An X-ray photon is produced when an electron from an adjacent shell drops to an inner shell to replace the ejected electron. Each element has its own set of characteristic X rays and therefore elements present in a sample can be identified by their wavelength or energy if a spectrum of emitted X rays is collected. That is the basis of X-ray microanalysis.

There are two types of X-ray detectors: the wavelength dispersive spectrometer (WDS) and the energy dispersive spectrometer (EDS). In WDS, a small portion of the emitted X rays hit a crystal. X rays that satisfy Bragg's law for the crystal are diffracted to a proportional counter. X-ray spectra are collected by varying the crystal type and its position on the focusing circle. The advantages of WDS are excellent energy resolution (avoiding elemental overlaps), lower limit of

detection (about 100 ppm instead of 1000 ppm), and high signal-to-noise ratio. However, WDS uses higher beam currents than EDS (more sample damage and larger probe size), and is very sensitive to surface roughness. Also, simultaneous multielement acquisition requires more than one detector.

Before EDS was introduced to SEM in 1968, X-ray microanalysis was primarily done with wavelength dispersive spectrometers using dedicated electron microprobes. EDS has poorer energy resolution than WDS (ca. 140 eV versus 20 eV), but the whole energy spectrum can be recorded simultaneously and therefore the elemental components can be quickly identified. Today, EDS detectors are commonly found on SEMs. In EDS, X rays pass through a thin window to a lithium-doped silicon crystal. The energy of incoming X rays is measured from the number of electron-hole pairs generated in the crystal by each X ray photon. A beryllium window (ca. 8 μm thick) usually separates the vacuum in the microscope from that around the liquid nitrogen cooled Si(Li) crystal. The beryllium (Be) window blocks out most X rays from elements lighter than atomic number 11 (sodium). Windowless and ultra-thin window detectors extend the range down to $Z = 4$ (Be). Since the 1990s, durable atmospheric thin windows (ATW) have been replacing Be windows, allowing full-time light element detection [*9*].

Accurate quantitative analysis requires careful control of conditions and an understanding of the beam interaction volume. In quantitative X-ray analysis with EDS, the X-ray intensities of each element in a sample are measured and compared to the measured intensities of well-characterized standards. The concentration of each element in the sample is the ratio of the X-ray intensity of each element in the sample to that in the standard. Still, corrections are needed to account for the different ways X rays are generated in the sample compared to the standard. These include backscattering and the stopping power (Z), X-ray absorption (A), and fluorescence (F). Together, these corrections are known as the ZAF correction. EDS analytical systems available from commercial vendors have computer programs that calculate ZAF corrections, or the alternative $\phi(\rho z)$ corrections [*9*]. Quantitative EDS analysis without standards has its limitations, but has been effectively applied [*10*].

In X-ray mapping a compositional image is created with elemental windows selected from an EDS or WDS detector. Labana and Wheeler [*11*] mapped the spatial distribution of elements in a corroding metal-coating interface of painted phosphated steel using an electron microprobe. Elemental concentrations were determined quantitatively from individual spot analyses using the wavelength dispersive detectors.

EDS elemental X-ray maps can be very useful in tracing production defects or failures in coatings. Figure 5 from Germani [*12*] shows a cross section of paint that was applied to a metal sign. The SEM/BSE image (upper left) reveals the location of the primer, white ink, and clear topcoat layers. The clear topcoat suffered delamination upon outdoor exposure. The failure at the ink-topcoat interface was attributed to chlorine migration into the clear coat from the ink (see the chlorine X-ray map). The titanium signal is from titanium dioxide pigment. Silicon in the primer may come from a mineral pigment and from a deglossing agent in the topcoat.

Crystal Orientation by SEM

Electron diffraction in the TEM is an established approach to the determination of crystal structure in electron microscopy. However, backscattered electrons in an SEM can also be used to generate diffraction patterns. As with X-ray diffraction and other forms of electron diffraction,

Bragg's Law controls the constructive interference of energy waves from a crystalline material. Electron diffraction from the focused beam on a polycrystalline sample generates light and dark Kikuchi bands containing information on the crystal orientation and identity. Reimer et al. [*13*] compared approaches such as high energy electron diffraction (HEED), electron channeling patterns (ECP), and electron backscatter diffraction (EBSD).

EBSD holds great potential for the study of coatings. The patterns come from within tens of nanometers of the surface [*14*]. They can be used to map the orientation of crystallites and their grain boundaries and to identify the crystalline phase. Modern EBSD systems include a tilted mount, retractable camera, and specialized software to enhance and analyze the patterns. Low-cost high-speed computers allow rapid automated calculations and integrated image displays.

Conductive Coatings

Historically, all electrically nonconductive materials have been given a thin conductive coating prior to SEM analysis. Application of a 10 to 20 nm coating, after mounting the sample on a conductive base, provides a pathway for electron flow to prevent charge buildup. Metal coatings also increase SE yield and signal strength, indirectly improving feature resolution. With the advent of variable pressure SEMs (VPSEMs) and the operation of SEMs at low accelerating potential, there are now some situations in which a conductive coating may not be needed at all.

For routine SEM imaging with secondary electrons, gold or gold-palladium coatings are applied. When the main objective is analysis using the X-ray or BSE detector, carbon coating may be more appropriate. Carbon has low X-ray (and electron) absorption and its low-energy characteristic X rays are normally not in the range of sample peaks. Metal coatings can generate their own X-ray background and characteristic peaks in critical ranges. They can also suppress the BSE contrast inherent in the specimen. Carbon coatings will generally not produce the level of feature resolution or charge dissipation obtained with metal coatings. Carbon is usually deposited by thermal evaporation under high-vacuum, but some low-vacuum methods are also available.

Coating techniques for SEM include thermal evaporation, plasma-magnetron sputtering, and DC glow discharge. Films are formed by thermal evaporation when a metal wire or carbon rod is heated to its melting point in a high vacuum ($<10^{-3}$ Pa). Films formed by thermal evaporation have large grains compared to other techniques and may not reach areas of the sample that are shadowed from this point source. As the resolution of SEMs improved, the grain size of metal coatings became a limit to resolution. Coating techniques that produce thinner, continuous films with smaller grains were needed. Plasma-magnetron sputtering is one of them.

In magnetron sputtering, films are formed when ionized, inert gas atoms strike a metal cathode to eject metal atoms, which deposit on the sample. Ionization efficiencies and, hence, sputtering rates are increased with an annular magnetic field that surrounds the cathode to concentrate electrons in the cathode area [*15*]. Films made with magnetron sputtering have smaller grains than thermally evaporated films. The magnetron sputter-coater is now standard equipment in most SEM labs. Care should be taken not to allow rotary-pumped coaters to reach their ultimate vacuum. Otherwise, pump oil can disrupt nucleation when it contaminates the target and the sample. State-of-the-art magnetron coaters are evacuated with oil-free turbomolecular pumps and equipped with cold stages because low sample temperatures decrease grain size. Au/Pd alloy targets produce finer grain coatings than pure gold, but some users avoid

them due to the additional peaks that appear during X-ray microanalysis.

Metal film thickness can be measured to ensure that only enough metal is deposited on the sample to form a continuous film. The quartz microbalance is the most widely used instrument to measure film thickness on electron microscopy specimens. Methods of film-thickness determination were discussed by Flood [*16*].

Extra care is required to coat samples with ultrathin (1 to 4 nm) continuous films needed to take advantage of the high resolution at magnifications over 50 000 times, available from FESEMs. Magnetron coaters made to accommodate a chromium target and a greater range of controls are commercially available. More recently, a method of osmium coating through DC glow discharge has proven to provide excellent high-resolution images [17]. The osmium tetroxide dissociates in the glow discharge and ionized osmium molecules form an amorphous metal film on the sample surface. Safety considerations for the toxic osmium tetroxide have been addressed in the design.

Sample Preparation and Cross Sections

If samples are not dry and a cryogenic or variable pressure SEM is not available, some method of stabilization and drying will be necessary. This might simply entail drying in an oven or vacuum oven. If such drying will alter the microstructure, then freeze-drying or critical point drying may be used. Other approaches include exchanging the solvent with epoxy or making a cast/replica of the surface. Dry samples are trimmed to a size adequate for the microscope stage and attached to a planchet (mount) with conductive paint or tape.

When cross-sectioning is needed for analysis of internal structure or composition, several methods are available. Sometimes a broken or fractured edge is sufficient. Cut faces are usually too rough or smeared to reveal essential features. If the material is soft or plastic, freeze-fracturing in liquid nitrogen may work. The best sections are usually prepared with a microtome or by grinding and polishing. Samples are normally embedded in epoxy prior to microtomy or metallographic polishing.

Microtomes are designed to cut sections of specified thickness ranges. Depending on the design, they may have metal, glass, or diamond knives. Rotary microtomes cut thick sections (ca. 20 μm) for light microscopy. Some ultramicrotomes have "thick" settings for sections approximately 2 to 10 μm thick, and "thin" settings for 50 to 200 nm TEM sections. Although microtomes do not generally work well on very hard materials, ultramicrotomes can be used to prepare ultrathin TEM sections of silicon wafers and ceramics [*18*]. For SEM, one only needs a cleanly cut block face, although the sections cut from it can be analyzed. Improved resins and microtomes have made cross-sectioning of paints less difficult. Derrick et al. [*19*] used glass knives in an ultramicrotome to produce 5 μm-thick paint sections.

Cross sections are often used to determine the thickness, composition, and structure of coating layers with SEM. Coated papers have historically been sectioned by microtome, but grinding and polishing have become more common due to improved procedures and the larger sample area exposed [*20*]. Figure 6 shows an SE image of a polished and etched section of coated paper with excellent detail. Sometimes BSE imaging is used to display the compositional contrast of coating layers and components. ASTM Test Method D 5235 [*21*] describes a grinding-polishing method for preparing and measuring cross sections of coatings on wood, using light microscopy. With modification, this procedure might be used for SEM, especially

VPSEMs that do not require dry specimens.

On the leading edge of cross-section technology is focused ion beam (FIB) preparation for TEM and SEM. These systems are quite expensive but have been extensively used in semiconductor analysis. Typically, the FIB workstation has a gallium ion source that is used to thin and shape a small area of interest. This method has enabled the production of well-resolved images of thin ink layers on printed paper [22].

Cryogenic SEM

Electron microscopes operating in the normal high-vacuum mode have a pressure lower than 10^{-3} Pa in their specimen chambers. This limits conventional SEM to dry samples. When volatile samples like paints are placed in the SEM specimen chamber their solvents quickly evaporate, contaminating the electron column, damaging the vacuum pumps, and causing the electron beam to scatter. One solution is to lower vapor pressures by freezing and examine samples in an SEM equipped with a stage cooled by liquid nitrogen. The technique is known as cryogenic SEM (cryo-SEM), described by Sheehan *[23-25]* for examining paper-coating formulations. The reader is also referred to Echlin *[26]* for more on techniques of cryo-electron microscopy.

The procedure of cryo-SEM is to fast-freeze each sample and transfer it into a vacuum chamber attached to the SEM specimen chamber. There each sample is fractured, sometimes etched, and then coated with a thin metal film. Then the sample is transferred to a cold stage in the SEM. The challenges of high-resolution cryo-SEM are to freeze fast enough to prevent noticeable growth of ice crystals, transfer without condensing water vapor on the fracture surfaces, coat frozen-hydrated samples with an ultrathin, continuous metal film, and image in the SEM without too much buildup of contaminants.

Wet microstructures of coating formulations can be examined with cryo-SEM after freezing and fracturing. Complementary fracture faces of a frozen-fractured pigment/latex coating formulation are shown in Figure 7. Kaolin and calcium carbonate particles can be identified by their morphologies. The dark areas between the particles are ice. Close examination of the complementary faces shows that fractures propagated around the pigment particles.

Environmental and Variable Pressure Scanning Electron Microscopy

Cryo-microscopy is one approach to imaging volatile samples in the SEM. Variable pressure SEM (VPSEM), including the environmental SEM (ESEM), is another. Before the advent of the ESEM, some laboratories cut back the vacuum level in the SEM sample chamber and imaged their materials exclusively with a backscattered electron detector. Usually a scintillator-type BSE detector was used because of its greater topographic contrast and better response at high scan speeds than solid-state detectors. In recent years, SEM vendors without access to the ESEM SE detector began to offer variable pressure capabilities on many microscope models, advertising a resolution of 5 nm in variable pressure mode.

A revolutionary development in SEM in the 1980s allows the imaging of wet, volatile specimens without freezing. It is known as environmental SEM (ESEM) [27]. With the ESEM, samples are imaged in a gaseous environment at pressures up to 2.7 kPa. This is made possible by a combination of a differentially pumped vacuum system, small travel distances for the

electron beam in high-pressure gas, and (most importantly) a biased current detector known as the gaseous secondary electron detector. The gas in the specimen chamber is a medium for SE signal multiplication and it neutralizes charge buildup on samples. Therefore, metal coating is not required for electrically insulating samples. ESEM resolution approaches that of a conventional SEM in SE mode. In order to obtain optimum resolution from electrically insulating samples a conductive coating may be needed to boost SE contrast.

The main advantage of ESEM compared to conventional SEM is that hydrated samples can be examined in their natural states at water-saturated vapor pressures. This makes possible dynamic imaging of wetting and drying by controlling sample temperature and water-vapor pressure. An ESEM image of paper, taken at 800 Pa of water vapor pressure and 20 °C, is shown in Figure 8A. Water was condensed on the same area by raising water vapor pressure to 1.3 kPa and lowering sample temperature to 12 °C. An image is shown in Figure 8B. Most of the fibers are covered with water. Other experimental gases can be used in the sample chamber instead of water.

A paper coating formulation with plastic pigment and a high latex content is susceptible to damage and difficult to image in a conventional SEM [*28*]. ESEM images in Figure 9 compare 0.10 μm plastic pigment in mixtures with 14% and 44% latex binder by weight. They show the packing of pigment particles and filling of interparticle pores. Few pigment-size pores are open at the 44% binder level.

Care must be taken with ESEM of hydrated specimens to avoid specimen damage by radiolysis products of water. Water molecules are radiolyzed by the electron beam into mainly hydrogen and hydroxyl radicals, which diffuse into specimens and sometimes damage them [*29,30*]. Also, the spread of the electron beam in the gaseous environment makes EDS spot analysis more difficult to control.

TRANSMISSION ELECTRON MICROSCOPY

The transmission electron microscope (TEM) produces images from electrons that have been transmitted through ultrathin sections of samples, or naturally thin particles. The spread of the beam in a sample is minimized by the thin specimen, allowing higher spatial resolution than SEM. Modern TEMs can resolve better than 0.2 nm. Contrast mechanisms include scattering, diffraction, and phase contrast. The useful thickness of amorphous samples at 100 kV is 100 to 3000 nm. For metal foils and crystalline materials at 100 kV, it is about 50 to 200 nm [*31*]. With added scanning transmission electron microscope (STEM) capabilities, compositional and structural data can be collected from a spot 1 nm or less in diameter.

Types of Contrast

Electron beam interactions that lead to contrast in the TEM are shown in Figure 1. In ultrathin samples, the beam does not spread into the teardrop shape shown for a bulk specimen. Electrons are elastically scattered by coulombic interactions with positively charged nuclei as they travel through TEM specimens. Scattering contrast is also known as amplitude contrast, or mass-thickness contrast, because the amount of scattering depends on specimen thickness and atomic number. Scattering contrast in TEM can be imaged in the bright-field mode and in the dark-field mode. In the bright-field mode, electrons that are scattered at larger angles are

intercepted by the objective aperture. Others pass through the objective aperture and form the image. In the dark-field mode, only the electrons that are scattered at large angles are used to form the image. This is accomplished by tilting the electron beam off axis or by moving the objective aperture off axis. In STEM, an annular dark-field detector collects that signal.

Another type of contrast caused by elastic scattering is known as phase contrast, the result of interference between the scattered and the unscattered electrons. Phase contrast varies as the objective lens focus is varied above or below the specimen. Diffraction contrast results when Bragg reflections from crystalline planes interfere with the primary beam. The interference image gives information about crystal structures.

Inelastic interactions in TEM include plasmon excitations and inner-shell ionizations. Some TEMs are equipped with electron spectrometers that measure the energy loss spectrum, known as electron energy loss spectroscopy (EELS). Electronic structures are indicated by plasmon losses, whose energies are less than 50 eV. Chemical compositions are indicated by losses from inner shell (K, L, and M) ionizations [*31*].

Optics

A schematic of an electron-optical column of a TEM is shown in Figure 10. It is similar to an upside-down view of a compound light microscope, with the illumination source being an electron gun. The electron-optical column of the TEM differs from the SEM in several ways. First, the electron beam is not scanned across the sample (except in STEM mode). The condenser lens system illuminates the entire area to be imaged. Second, the TEM has a projector lens system that focuses the transmitted electrons onto a phosphor screen, where the image can be viewed. Third, higher accelerating potentials (80 to 500 kV) in TEM are needed to transmit electrons through thin samples. Accelerating potentials in SEMs range from about 300 V up to 30 kV.

The two condenser lenses work together in the normal TEM imaging modes. The first condenser lens (C1) controls the spot size, while the second condenser lens (C2) is used to adjust brightness. In the STEM mode, where a finely focused probe is required, C2 is essentially turned off, and the upper part of the objective lens is used as a third condenser lens to focus the beam.

The objective lens forms, focuses, and initially magnifies the image. In most TEMs the specimen is inserted into the objective lens section of the column. The objective aperture blocks scattered electrons in the bright-field mode, discussed above. Contrast is increased if a smaller objective is selected, but the signal strength will decrease accordingly.

The projector lens system projects the transmitted electrons onto the phosphor viewing screen or photographic emulsion. A wide variety of digital cameras are now available for image collection below the column or through a side-mounted camera port. Digital image collection gives the operator immediate feedback on results, avoiding darkroom processing time.

ADDITIONAL COATING APPLICATIONS

Pigment Particle Size and Identification

There are numerous non-microscopic methods for determining particle size distribution. Given a large, well-dispersed pigment population, these automated methods generate statistically

valid measurements in very little time. Each approach, including microscopy, measures "size" differently and is likely to generate somewhat different results. Microscopic size measurement is a powerful approach when the shapes of particles need to be determined or when they are fixed in a dry coating. Particle-size measurements are more fully explored in a separate chapter of this manual.

The microscope is especially useful for measurement of plate-like and needle-shape particles that do not obey Stokes' law on which the sedimentation methods are based. However, microscopic methods can be slow and laborious. In the past, particle-size analysis was performed by manually measuring particles with the aid of a reticle or grid on the microscope display or with a ruler using printed micrographs. Today, with size-calibrated digital images collected on electron microscopes, selected dimensions can be easily measured with the click of a mouse. Automated image analysis is possible if individual particles can be made to stand out unambiguously from their background by a combination of the right sample preparation, signal selection, and image processing. It must be understood that the particle images represent two-dimensional projections or slices of three-dimensional objects. True diameters may not be presented, and preferred orientation of particles in a coating will affect their shape within the section.

Pigments of known morphologies can be identified easily with both SEM and TEM. Some pigment particles are smaller than 0.1 μm and therefore conductive coatings must be ultrathin in order not to blanket morphologies of the particles before SEM imaging. Pigment particles can also be identified in SEM by their EDS spectra if the particles are larger than a few micrometers. Identification of smaller particles in SEM with an EDS is hampered by the large generation volume of X rays.

Figure 11 shows images of kaolin clay taken with SEM (Figure 11A) and TEM (Figure 11B). The different contrasts in the SE mode with the SEM and in the bright-field mode with TEM are clear. The SE contrast is topographical and the TEM contrast depends on mass-thickness. In both, the pseudohexagonal, plate-like habits of particles are indicators of the presence of kaolin.

Contact diameters of various sizes of latex have been measured with SEM [*32*] and TEM [*33*] and compared to theoretical predictions. Demejo et al. [*34*] imaged with high-resolution SEM extents of latex deformation resulting from particle-substrate adhesion and compared their results to theoretical predictions.

Failures and Defects

Pits, cracks, and loss of adhesion can be readily examined with SEM. Some contaminants can be identified by their morphologies and others by their characteristic X rays using EDS. Here are some examples: SEM examination of a paint film that failed rapidly in a salt spray test revealed a textured surface that rusted rapidly in the pitted areas. When the paint was applied with a smooth finish, it passed the salt spray test. Poor scrubbability in a latex paint was due to lack of coalescence, readily apparent after SEM examination revealed many cracks in the film. Loss of adhesion on metal reflectors was due to insect eggs which pulled the paint off as the eggs dried. A glossy varnish which turned out flat was found to be laden with diatomaceous earth from a broken filter [*35*].

Quach [*36*] used SEM with EDS to identify contaminants responsible for adhesive failures.

Welding splatter was identified as a cause of chipping of paint on a steel building chord. EDS was also used to identify plaster dust, fly ash, and sulfur dioxide as contaminants that caused adhesive failure in other samples.

Structure and Wear

Bishop and Silva [*37*] examined leaching of pigment in cross sections of antifouling paint films. Cross sections were made by fracturing in liquid nitrogen. They found a linear correlation between the leached matrix thickness and the volume fraction of pigment. Examination of complimentary fracture faces was required to see if leached pigment or fracture was responsible for voids. They also showed that the insoluble matrix of microtome-sectioned films was distorted.

SEM examination of weathered paint films showed the onset of chalking when binder wears away from between pigment particles [*38,39*]. However, the conclusion was that SEM images point to the cause of chalking, but gloss measurements are a more quantitative and economical method for routine weatherability evaluation.

Nylon coatings are used in such applications as printing rollers and marine hardware because of their wear and weather resistance. Thermally sprayed nylon 11 coatings with 7 and 12 nm silica pigment were sectioned and analyzed by SEM [*40*]. SEM was used to determine the structure of the raw materials and finished coating. Cross-section images, supported by EDS, showed nylon polymer cells surrounded by bead-like silica-rich interfaces.

ACKNOWLEDGMENTS

Sincere thanks go to the member companies of IPST for supporting the work of the first author.

REFERENCES

[*1*] McMullan, D., "SEM-Past, Present and Future," *Journal of Microscopy*, Vol. 155, No. 3, 1989, pp. 373–392.

[*2*] Princen, L. H., Ed., "Scanning Electron Microscopy of Polymers and Coatings," May 27-28, 1970, ACS Symposium, *Applied Polymer Symposia*, No. 16, John Wiley and Sons, New York, 1971.

[*3*] Princen, L. H., Ed., "Scanning Electron Microscopy of Polymers and Coatings II," April 8-13, 1973, ACS Symposium, *Applied Polymer Symposia*, No. 23, John Wiley and Sons, New York, 1974.

[*4*] Thomas, E. L., "Electron Microscopy," *Encyclopedia of Polymer Science and Engineering*, Vol. 5, John Wiley and Sons, New York, 1986.

[*5*] Goldstein, J. I., Newbury, D. E., Echlin, P., Joy, D. C., Romig, A. D., Lyman, C. E., Fiori, C., and Lifshin, E., *Scanning Electron Microscopy and X-ray Microanalysis*, Second Edition, Plenum Press, New York, 1992.

[*6*] Reimer, L., *Scanning Electron Microscopy*, Springer Verlag, New York, 1985.

[*7*] Boyes, E. D., "On Low Voltage Scanning Electron Microscopy and Chemical Microanalysis," *Microscopy and Microanalysis*, Vol. 6, No. 4, 2000, pp. 307-316.

[*8*] Peters, K. R., "Conditions Required for High Quality High Magnification Images in Secondary Electron-I Scanning Electron Microscopy," *SEM 1982*, Vol. IV, SEM, Inc., Chicago, 1982, pp. 1359–1372.

[*9*] Friel, J. J. and Mott, R. B., "Energy-Dispersive Spectrometry from Then until Now: A Chronology

of Innovation," *Microscopy and Microanalysis*, Vol. 4, No. 6, 1999, pp. 559-566.

[*10*] Newbury, D. E. "Standardless Quantitative Electron-Excited X-ray Microanalysis by Energy-Dispersive Spectrometry: What is the Proper Role?" *Microscopy and Microanalysis*, Vol. 4, No. 6, 1999, pp. 585-597.

[*11*] Labana, S. S. and Wheeler, M., "Characterization of Coatings by Electron Microprobe Analysis," *Scanning Electron Microscopy of Polymers and Coatings II*, L. H. Princen, Ed., John Wiley and Sons, New York, 1974, pp. 61–72.

[*12*] Germani, M. S., "Scanning Electron Microscopy & Coatings Analysis," *Paint & Coatings Industry Magazine*, Vol. 14, No. 6, 1998. pp. 102-115.

[*13*] Reimer, L., Heilers, U., and Saliger, G., "Kikuchi Band Contrast in Diffraction Patterns Recorded by Transmitted and Backscattered Electrons," *Scanning*, Vol. 8, No. 3, 1986, pp. 101-118.

[*14*] Dicks, K., "Crystal Orientation Mapping of Copper Interconnects using EBSD," *Microscopy Today*, Vol. 00-6, 2000, pp. 36-38.

[*15*] Nockolds, C. E., Moran, K., Dobson, E., and Phillips, A., "Design and Operation of a High Efficiency Magnetron Sputter Coater," *SEM 1982*, Vol. III, SEM, Inc., Chicago, 1982, pp. 907–915.

[*16*] Flood, P. R., "Thin Film Thickness Measurements," *SEM 1980*, Vol. I, 1980, SEM, Inc., Chicago, pp. 183–200.

[*17*] Tanaka, A., "Osmium Conductive Metal Coating for SEM Specimen Using Sublimated Osmium Tetroxide in Negative Glow Phase of DC Glow Discharge," *J. Electron Microscopy*, Vol. 43, No. 4, 1994, pp. 177-182.

[*18*] Malis, T.F. and Steel, D., "Ultramicrotomy for Materials Science," *Workshop on Specimen Preparation for TEM of Materials II*, R. Anderson, Ed., Materials Research Symposium Proceedings, Materials Research Society, Pittsburgh, PA, Vol. 199, 1990.

[*19*] Derrick, M., Souza, L., Kieslich, T., Florsheim, H., and Stulik, D., "Embedding Paint Cross-Section Samples in Polyester Resins: Problems and Solutions," *J. American Institute for Conservation*, Vol. 33, No. 3, 1994, pp. 227-245.

[*20*] Williams, G. J. and Drummond, J. G., "Preparation of Large Sections for the Microscopical Study of Paper Structure," *J. Pulp Paper Science*, Vol. 26, No. 5, 2000, pp. 188-193.

[*21*] American Society for Testing and Materials, "D 5235-97, Standard Test Method for Microscopical Measurement of Dry Film Thickness of Coatings on Wood Products," *Annual Book of ASTM Standards*, ASTM International, West Conshohocken, PA, Vol. 6.02, 2002.

[*22*] Uchimura, H., Ozaki, Y., and Kimur, M., "Sample Preparation Method for Printed Paper Cross-sections using focused ion beam," *Proceedings of the International Printing and Graphic Arts Conference*, TAPPI Press, Atlanta, 1998, pp. 121–124.

[*23*] Sheehan, J. G., "A Conduction-Cooled Stage for High Resolution Cryo-SEM," *Proceedings of the 50th Annual Meeting of the Electron Microscopy Society of America*, San Francisco Press, 1992, pp. 1282–1283.

[*24*] Sheehan, J. G., "A Metal-Coating Chamber for High Magnification Cryo-SEM," *Proceedings of the XIIth International Congress for Electron Microscopy*, San Francisco Press, 1990, pp. 418–419.

[*25*] Sheehan, J. G. and Whalen-Shaw, M., "High Magnification Cryogenic Scanning Electron Microscopy (Cryo-SEM) of Wet Coating Microstructures," *TAPPI Journal*, Vol. 73, No. 5, 1990, pp. 171–178.

[*26*] Echlin, P., *Low-Temperature Microscopy and Analysis*, Plenum, New York, 1992.

[*27*] Danilatos, G. D., "Review and Outline of Environmental SEM at Present," *Journal of Microscopy*, Vol. 162, No. 3, 1991, pp. 391–402.

[*28*] Xiang, Y., and Bousfield, D. W., "Influence of Coating Structure on Ink Tack Dynamics," *J. Pulp Paper Science*, Vol. 26, No. 6, 2000. pp. 221-227.

[*29*] Sheehan, J. G., "Radiation Damage to Cellulose Fibers in ESEM," *Proceedings of the 49th Annual Meeting of the Electron Microscopy Society of America*, San Francisco Press, 1991, pp. 1130–1131.

[30] Sheehan, J. G., "Assessment of Environmental Scanning Electron Microscopy for Coating Research," *1991 TAPPI Coating Conference*, TAPPI Press, Atlanta, 1991, pp. 377–383.

[31] Reimer, L., *Transmission Electron Microscopy*, Springer-Verlag, New York, 1984.

[32] Eckersley, S. T. and Rudin, A., "Mechanism of Film Formation from Polymer Latexes," *Journal of Coatings Technology*, Vol. 62, No. 780, 1990, pp. 89–100.

[33] Kendall, K. and Padget, J. C., "Latex Coalescence," *International Journal of Adhesion and Adhesives*, July 1982, pp. 149–154.

[34] Demejo, L. P., Rimai, D. S., and Bowen, R. C., "Direct Observations of Deformations Resulting from Particle-Substrate Adhesion," *Journal of Adhesion Science and Technology*, Vol. 2, No. 5, 1988, pp. 331–337.

[35] Lind, W. K., *ASTM Paint and Coatings Testing Manual*, Ch. 10.1, ASTM, Philadelphia, 1971, pp. 515–521.

[36] Quach, A., "Applications of Energy-Dispersive X-ray Spectrometry in Interfacial Coating Failures," *Scanning Electron Microscopy of Polymers and Coatings II*, L. H. Princen, Ed., John Wiley and Sons, New York, 1974, pp. 49–59.

[37] Bishop, J. H. and Silva, S. R., "Antifouling Paint Film Structure, with Particular Reference to Cross Sections," *Scanning Electron Microscopy of Polymers and Coatings*, L. H. Princen, Ed., John Wiley and Sons, New York, 1971, pp. 195–208.

[38] Carter, O. L., Schindler, A. T., and Wormser, E. E., "Scanning Electron Microscopy for Evaluation of Paint Film Weatherability," *Scanning Electron Microscopy of Polymers and Coatings II*, L. H. Princen, Ed., John Wiley and Sons, New York, 1974, pp. 13–25.

[39] Princen, L. H., Baker, F. L., and Stolp, J. A., "Monitoring Coating Performance Upon Exterior Exposure," *Scanning Electron Microscopy of Polymers and Coatings II*, L. H. Princen, Ed., John Wiley and Sons, New York, 1974, pp. 27–40.

[40] Petrovicova, E., Knight, R., Schadler, L. S., and Twardowski, T. E., "Nylon 11/Silica Nanocomposite Coatings Applied by the HVOF Process. I. Microstructure and Morphology," *J. Applied Polymer Science*, Vol. 77, 2000, pp. 1684-1699.

TABLE 1--Performance parameters for electron sources [a]

	Tungsten	Lanthanum Hexaboride	Cold Field Emission	Schottky Thermal Field Emission
Gun Vacuum, Pa	10^{-3}-10^{-4}	10^{-5}	10^{-8}	10^{-7}
Lifetime, hours	50-100	≥1000	thousands	thousands
Source Size	50 μm	10 μm	2 nm	20 nm
Brightness, A/cm^2-sr	10^5	10^6	10^8	10^8
Signal Stability, (% drift/hour)	1	2	5 [b]	1-2
Maximum Probe Current, A	2 x 10^{-5}	2 x 10^{-5}	5 x 10^{-9}	5 x 10^{-7}
Energy Spread, electron-volts	2	1	0.1	0.2
SE resolution @ 30 kV, nm	3.5	2.5	0.5	1

[a] Approximate values. Adapted from sources including Goldstein et al. [5].
[b] Stability commonly improved by correction circuitry.

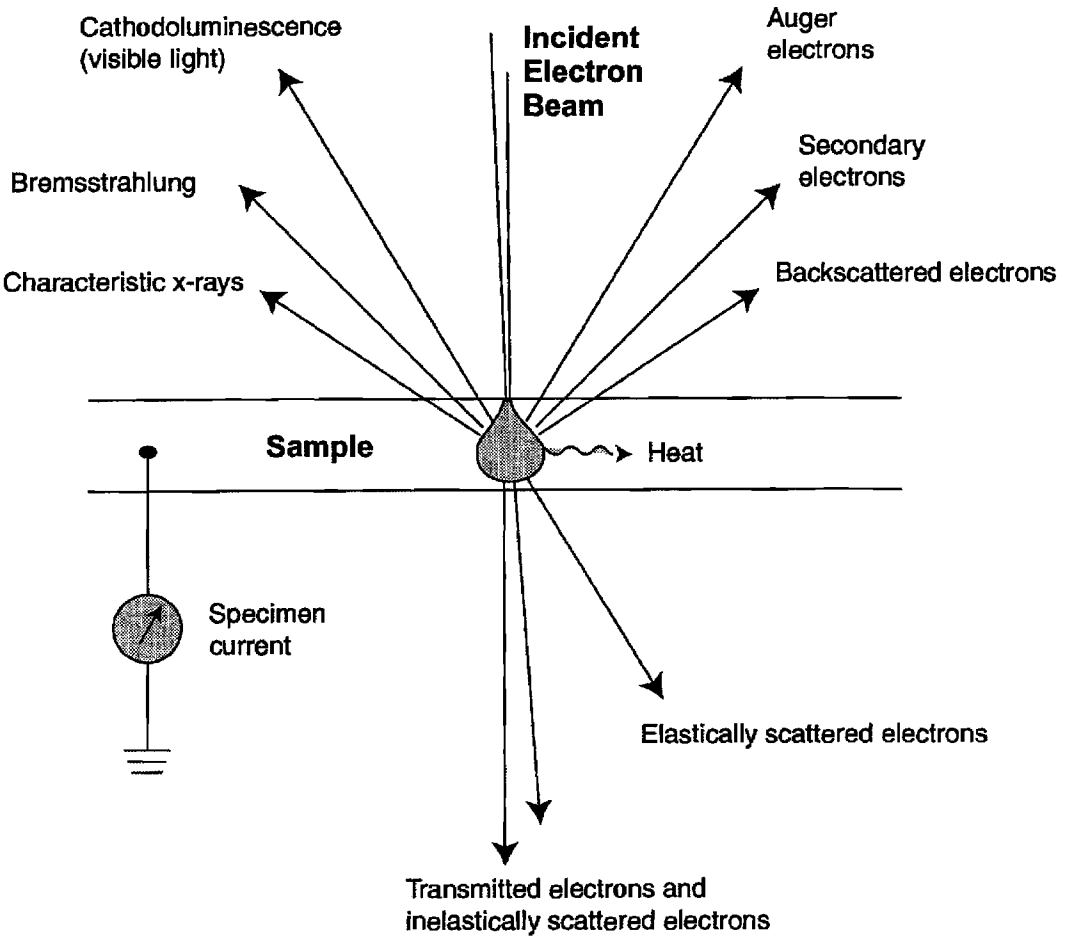

FIG. 1—Electron beam interactions with a sample and signal types generated. A typical thick SEM sample will have the teardrop-shaped interaction volume. Reproduced with permission from Thermo NORAN, a Thermo Electron business.

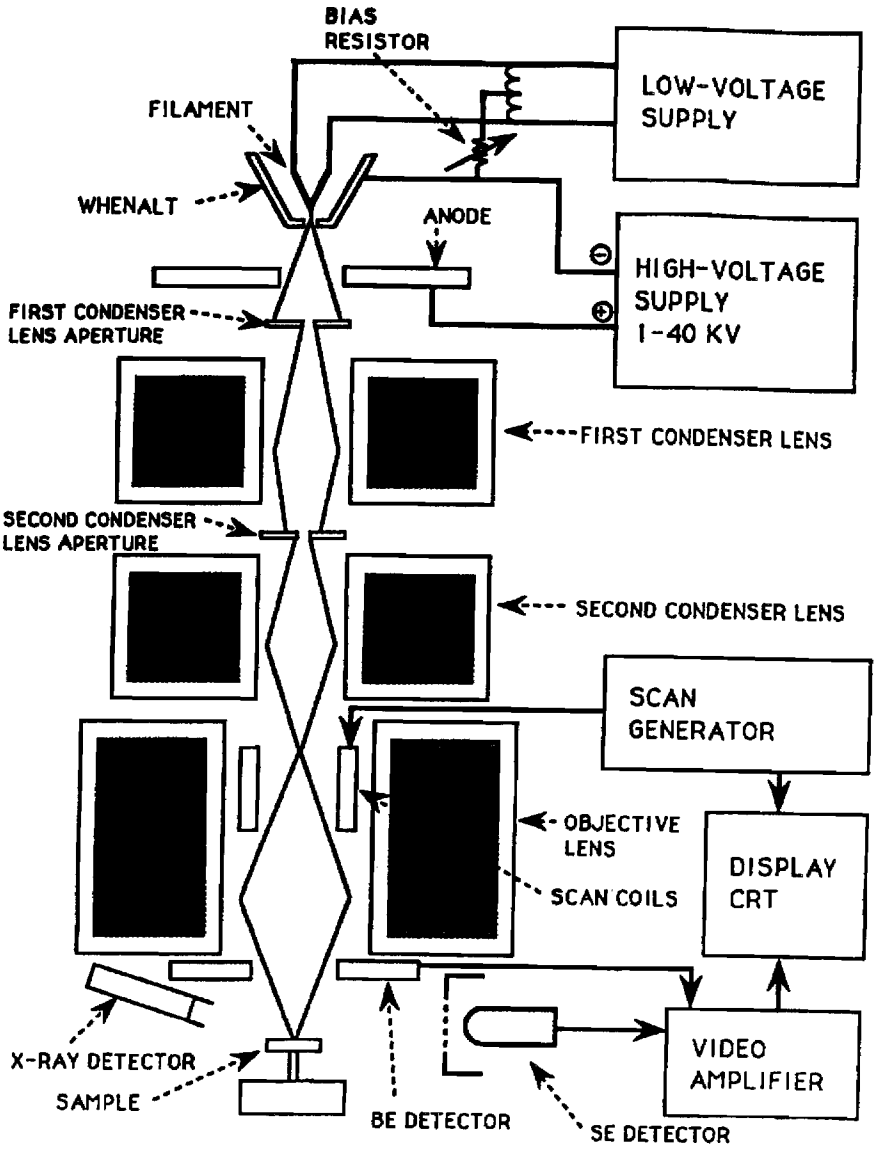

FIG. 2—Schematic diagram of an SEM with a thermionic electron gun. The "objective" lens is actually a final condenser lens. Adapted from Thomas [*4*].

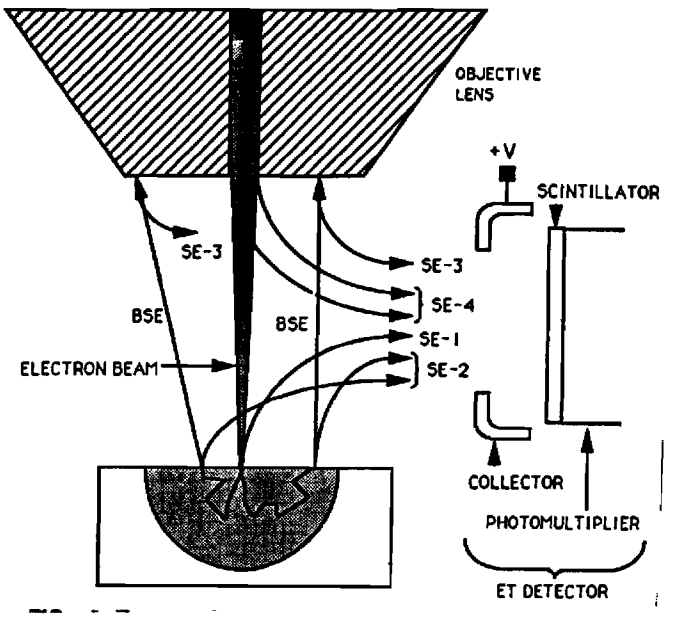

FIG. 3—Types of secondary electrons collected by the Everhart-Thornley detector. SE1 carries high-resolution topographic information. Adapted from Reimer [*6*].

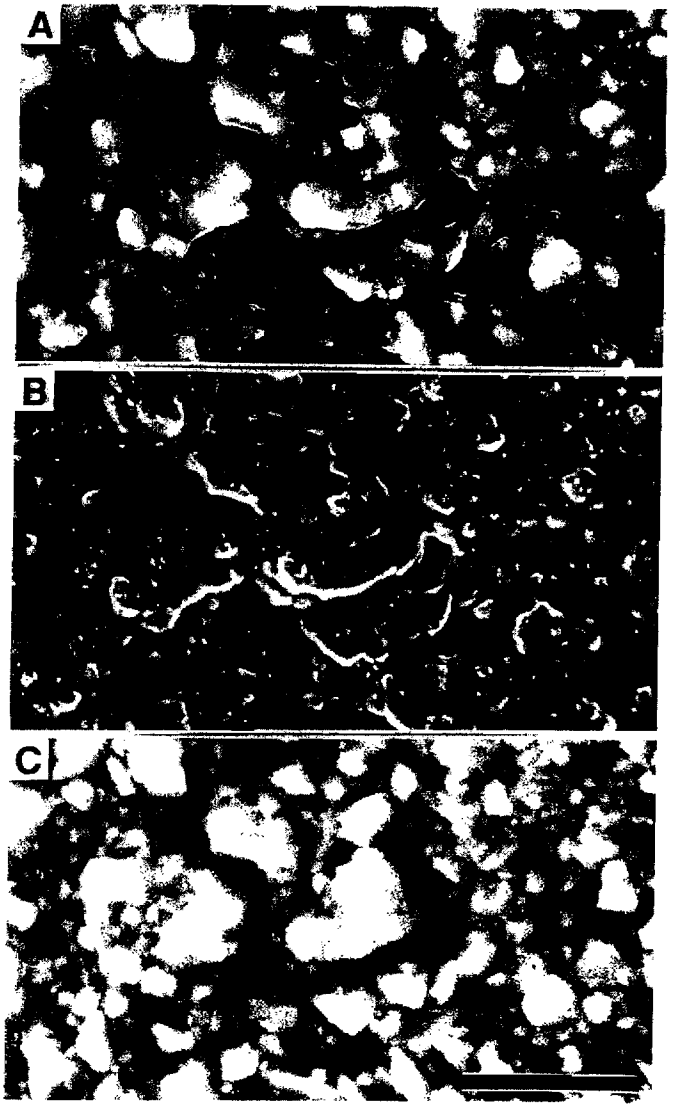

FIG. 4—Three SEM images of the same area of a coating formulation with 1:6 latex to calcium carbonate. Air dried from 80 wt% aqueous suspension. (A) SE image at 20 kV; (B) SE image at 5 kV; (C) BSE image at 20 kV. Bar = 10 μm.

FIG. 5—SEM/BSE image and three elemental x-ray maps of a paint cross section. Bar = 10 μm. Reproduced with permission from M. S. Germani [*12*].

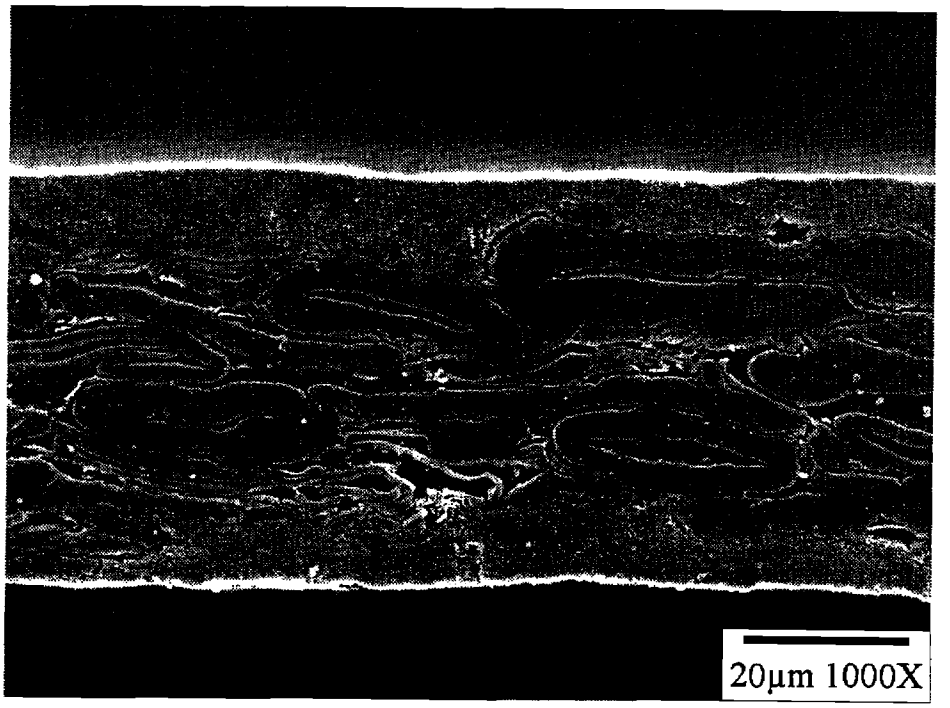

FIG. 6—Polished and etched cross section of lightweight clay-coated paper. Secondary electron SEM image. Bar = 20 µm. Photo by G. Maghiari, IPST.

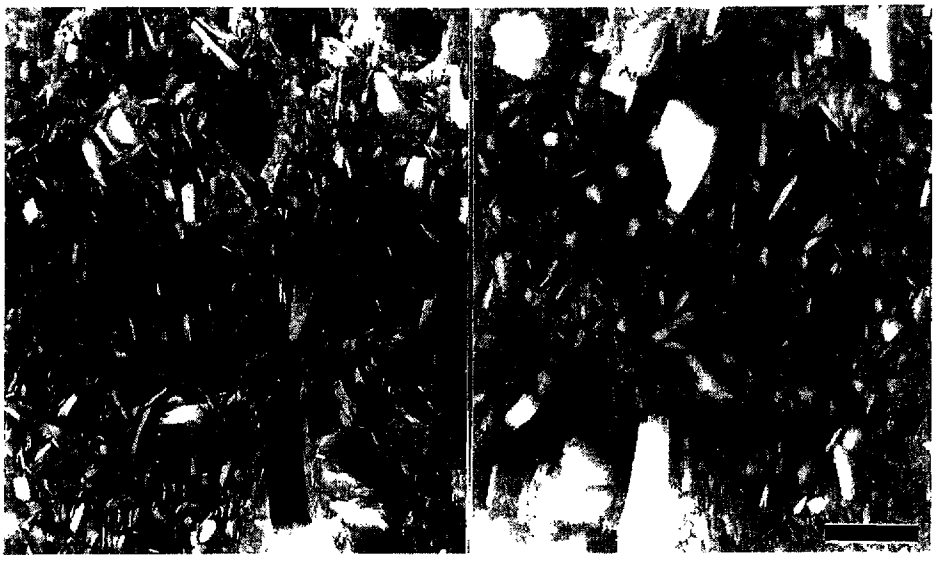

FIG. 7—Cryo-SEM image of complementary fracture faces of a coating formulation. Bar 1 μm [*24*].

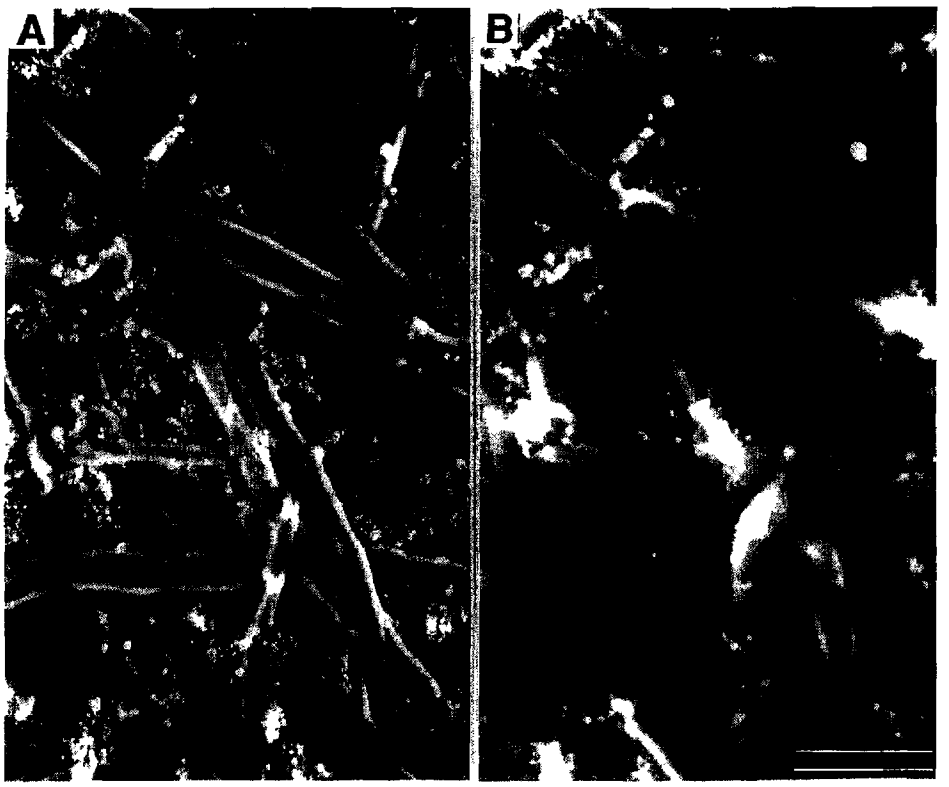

FIG. 8—Two ESEM micrographs of the same area of paper (A) before wetting; (B) wet Bar = 50 μm.

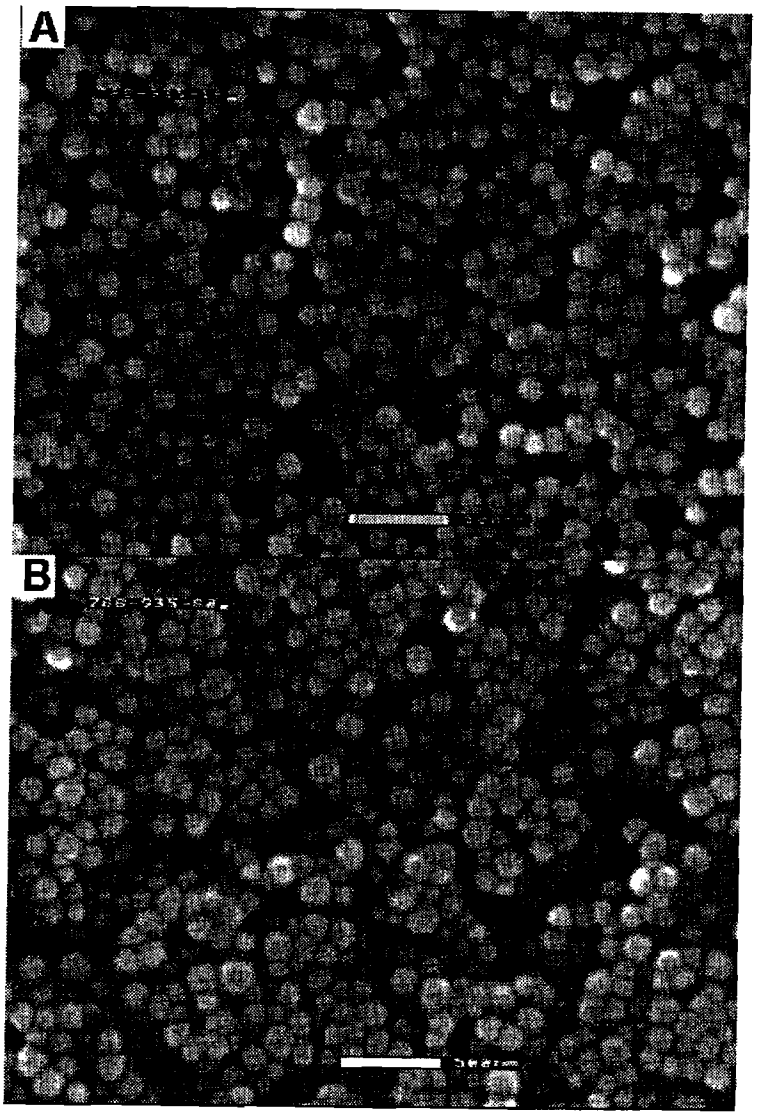

FIG. 9—ESEM micrographs of two coatings containing 0.10 μm plastic pigment with latex levels of (A) 14 wt%; (B) 44 wt%. Bar = 500 nm. Reproduced from Xiang and Bousfield [*28*] with permission from JPPS.

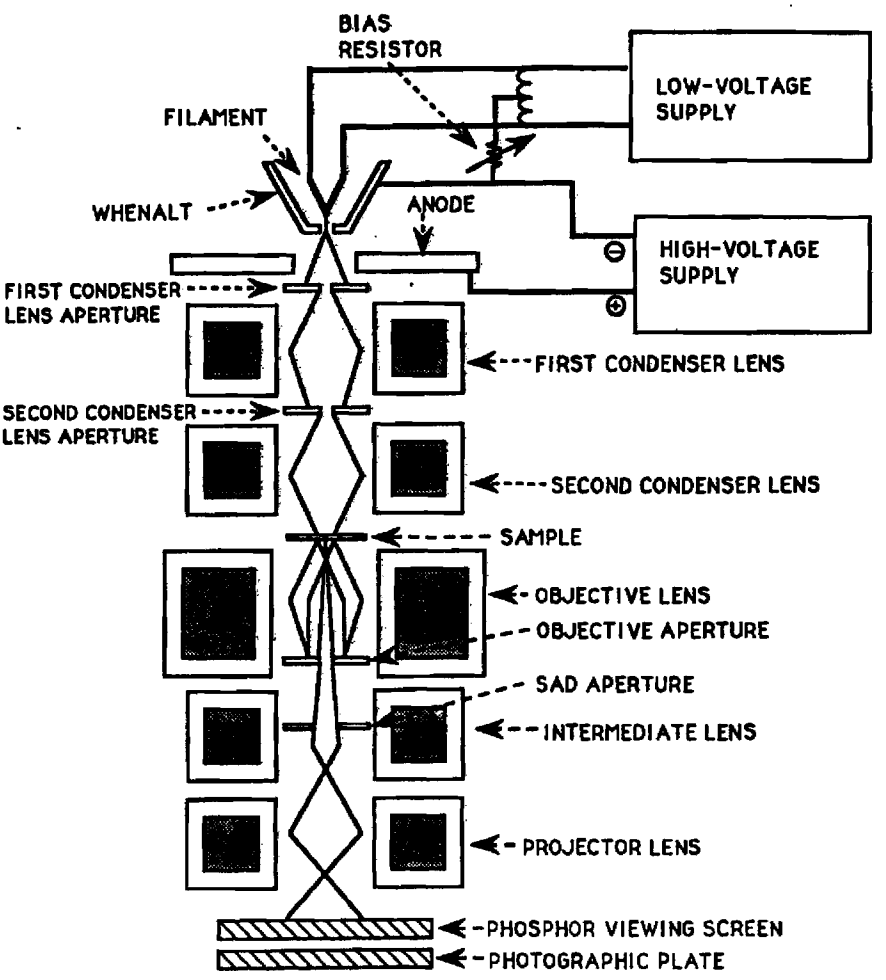

FIG. 10—Electron-optical column of the TEM. Adapted from Thomas [*4*].

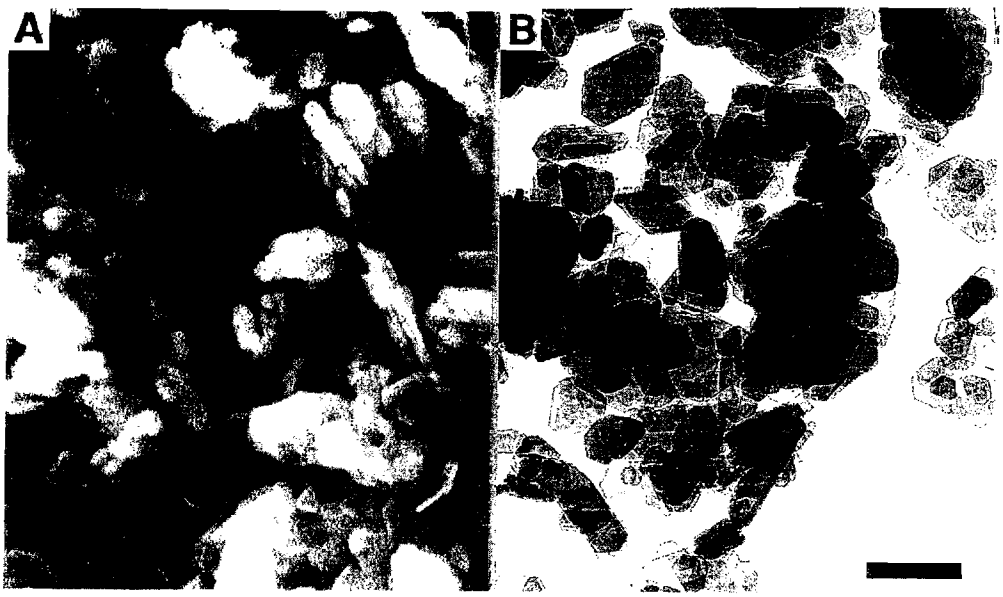

FIG. 11—Kaolin clay imaged in (A) SEM; (B) TEM. Bar = 0.5 μm. Photo by R. P. Gursky, Unilever Research.